Science Arts & Métiers (SAM)

is an open access repository that collects the work of Arts et Métiers Institute of Technology researchers and makes it freely available over the web where possible.

This is an author-deposited version published in: https://sam.ensam.eu
Handle ID: .http://hdl.handle.net/10985/8199

To cite this version :

Rafik HAJRYA, Nazih MECHBAL - Principal component analysis and perturbation theory–based robust damage detection of multifunctional aircraft structure - Structural Health Monitoring - Vol. 12(, n°3, p.263–277 - 2013

Any correspondence concerning this service should be sent to the repository Administrator : scienceouverte@ensam.eu

Arts et Métiers Institute of Technology

Principal Component Analysis and Perturbation Theory Based Robust Damage Detection of Multifunctional Aircraft Structure

Rafik Hajrya and Nazih Mechbal

Process and Engineering in Mechanics and Materials Laboratory (PIMM) CNRS-UMR 8006-Arts et Métiers ParisTech (ENSAM)

Address: 151 Boulevard de l'hôpital, 75013, Paris, France

Corresponding authors: Tel:+33 144246458

E-mail: rafik.hajrya@ensam.eu, nazih.mechbal@ensam.eu

Abstract

A fundamental problem in structural damage detection is to define an efficient feature to calculate a damage index (DI). Furthermore, due to perturbations from various sources, we need also to define a rigorous threshold whose overtaking indicates the presence of damages. In this paper, we develop a robust damage detection methodology based on Principal Component Analysis (PCA). We present first an original DI based on the projection on the separation matrix, and then we drive a novel adaptive threshold that doesn't rely on statistical assumptions. This threshold is analytic and is based on matrix perturbation theory (MPT). The efficiency of the method is illustrated using simulations on a composite smart structure with PZT and experimental results performed on a Conformal Load-Bearing Antenna Structure (CLAS) laboratory test.

Keywords: *Damage detection, blind source separation, principal component analysis, information theory, angle between subspaces, matrix perturbation theory, analytic bound, robustness, Conformal Load-Bearing Antenna Structure, temperature effect.*

Nomenclature

CLAS	=	Conformal Load-Bearing Antenna Structure
MAS	=	Multifunctional Aircraft Structure
BSS	=	Blind Source Separation
PCA	=	Principal Component Analysis
SVD	=	Singular Value Decomposition
MPT	=	Matrix Perturbation Theory
FPA	=	False Positive Alarm
ULM	=	Unsupervised Learning Mode
DI_{PCA}	=	Damage index based on PCA
$\mu_{\beta,PCA}$	=	Mean value of the bound
n_y	=	Number of sensors of the smart structure
N	=	Number of samples
$\underline{\boldsymbol{y}}(k)$	=	Measurements vector at instant k
$\underline{\boldsymbol{s}}(k)$	=	Sources vector at instant k

$\underline{\boldsymbol{r}}(k)$	=	Estimated sources vector
$\mathbf{Y}$	=	Measurements matrix
$\mathbf{T}$	=	Mixing matrix
$\mathbf{W}$	=	Separation matrix
$\mathbf{W}$	=	Transpose of matrix $\mathbf{Y}$
$\mathbf{Y}^s$	=	Measurements matrix of the structure in a healthy state
$\widetilde{\mathbf{Y}}^s$	=	Measurements matrix of a second experiment
$\mathbf{Y}^u$	=	Measurements matrix of the structure at unknown state
$\delta\mathbf{Y}^s$	=	Matrix which reflect the effect of disturbances
$\mathbf{U}$	=	Matrix of left singular vectors
$\mathbf{V}$	=	Matrix of right singular vectors Variance
$\underline{\boldsymbol{\psi}}$	=	Matrix of right singular vectors Variance
σ^2	=	Matrix of right singular vectors Variance
λ	=	Eigenvalue
η and δ	=	Numbers associated to the matrix perturbation theory (subsection 3.3)

1. *Introduction*

The aerospace industry is aiming, more than ever, to reduce their energy consumptions and emissions. Despite recent advances in aircraft engines, the determinant energy-saving factors are reducing weight and optimizing the aerodynamic performances. Moreover, the aerospace companies have also to satisfy safety constraints, structural integrity (mechanical stiffness and strength) and some customer requests (integration new features as for example, multimedia and private communications). As shown in figure 1, a present commercial aircraft is composed of many antennas located on the structure and used for communication, navigation and radar activity. Furthermore, in a near future, the number of these antennas is expected to increase in order to improve comfort customers by allowing multimedia private communications and internet accesses. Taken into account of these customer requests will result into to an increase of weight, and a decrease in the aerodynamic performances due to the huge number of antennas that will protrude from the outer mould line (OML) of the aircraft.

To respond to these antagonist criteria, ongoing research and development programs have come up with the concept of multifunctional aircraft structure (MAS). The principle is to take the advantage of composite materials to integrate airframe structure with a functional system. The objective is to perform a number of tasks such as transmit/receive (T/R) function, structural health monitoring (SHM), active control [1], shape control and Conformal Load-Bearing Antenna Structure (CLAS) [2;3]. The concept of CLAS is to replace existing antennas, particularly blades and wires that protrude from the OML of aircraft with airframe structure, that: (i) supports primary structural loads, (ii) conforms to the OML and (iii) can

perform the transmit/receive function of the existing antennas [4]. CLAS will then reduce drag and have the potential to reduce weight and enhance the electromagnetic performance.

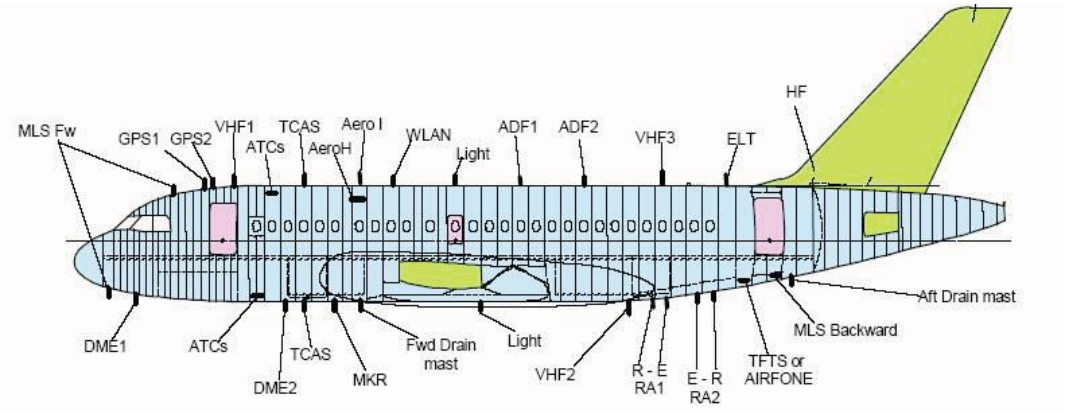

Figure 1: Antenna of the AIRBUS A318 [5]

However, the electromagnetic performances of this CLAS depend of their structural health, which can be clobbered by mechanical stress, impact damage or by delamination of a part of the antenna network from the host structure. Therefore, monitoring the health of the CLAS is a mandatory necessity.

In this paper, a methodology is proposed to achieve SHM on a CLAS composite structure. Our study is a part of a more global project (Smart Materials and Structures for Electromagnetics, MSIE) supported by the Aerosapce Paris Région [5]. The MSIE project aims to demonstrate the practical use of metamaterials in CLAS and to monitor their performances by performing in the case of damage, SHM for restorative maintenance tasks and shape control compensation.

SHM is the most widely known form of MAS. It has been driven by recent developments in sensor technology [6], manufacturing, signal processing [7], applied mechanics and material sciences. SHM has led to a variety of efficient methods to detect, locate, classify, quantifying varying degrees of damage and estimating the remaining useful life of the structure [8]. Several techniques have been employed to perform structural monitoring [9], and various damage indices have been proposed to characterize the change in dynamic characteristics caused by damage. Some of these DIs are based on extracting features from the observed output vector $\underline{\boldsymbol{y}}(t)$, using numerous tools such as short Fourier transform [10], wavelet [11] and Hilbert-Huang transform [12].

To perform SHM, the structure has to be smart. Smartness supposes spatial information which is obtained by network of sensors/actuators built in/on the host structure. This spatial diversity are achieved through multivariate and magavariate analysis to reduce data and to extract some

simplified and hidden pattern [13-15]. As the name implies, multivariate analysis is concerned with the analysis of multiple variables or measurements, but treats them as a single entity. Blind separation source (BSS) is a family of techniques, which belong to multivariate statistics. BSS attempts to reveal hidden variables, named sources $\underline{\boldsymbol{s}}$ and mixing/separating matrices, only from their dynamical measured vectors $\underline{\boldsymbol{y}}$. Among the methods of the BSS family, one can cite: Principal Component Analysis (PCA) [16], Independent Component Analysis (ICA) [17], Second-Order Blind Identification (SOBI) [18]. In this paper, we focus on PCA.

PCA has been used to extract damage features. Friswell and Inman [13] proposed a damage index based on the angle between subspaces. [14] have used the same approaches to detect a piezoelectric faulty sensor. Recently, [19] have explored the use of PCA and T^2 and Q-statistics to detect damage.

The key issue in damage detection is to ascertain with confidence if damage is present even if the structure is subject to environmental perturbations. In the above references, the threshold associated to the proposed damage indices are defined manually [19], or following the assumption of Gaussian distribution of the damage index [20].

In this study, we propose to develop a new robust analytical threshold (bound) that handle the effect of noise measurements, temperature changes and ensure the presence of damage. Our approach uses singular value decomposition (SVD) and matrix perturbation theory (MPT). MPT considers how the features of a matrix namely singular values, singular vectors and subspaces change, when the matrix is subject to perturbations [21]. In the proposed approach, we study perturbations that could rise in the subspaces of the separation matrix to define an analytic threshold to the damage index proposed in this paper.

The remainder of this paper is organized as follows. In preliminary, we introduce the BSS problem and the principal component analysis technique. In section 3, the damage detection procedure is described, and it is divided into four subsections; the first and second subsections are devoted respectively toward the development of feature extraction and our proposed damage index; in subsection 3.3, we present our new approach to define the threshold. We outline in subsection 3.4 a framework. In section 4, finite element simulation's results on a composite plate are presented. In section 5, we present the experimental study of a conformal load-bearing antenna structure (CLAS), and the damage detection results are presented in section 6. Finally, conclusions and further directions will be drawn in section 7.

2. *BSS problem and PCA algorithm*

2.1. *BSS problem*

In blind source separation, the goal is to recover unknown source signals $s_i(k)$ from their linear measured mixtures $\underline{\boldsymbol{y}}(k)$ without any information on the mixing coefficients [18]. We suppose in the sequel a linear mixture. Hence, let $\underline{\boldsymbol{y}}(k)$ be a zero mean measurement vector from n_y sensors at time index k:

$$\underline{\boldsymbol{y}}(k) = \left[y_1(k) \ \dots y_{n_y}(k)\right]^T \tag{1}$$

The measurement matrix $\mathbf{Y} \in \mathbb{R}^{n_y \times N}$ gathering N samples $\underline{\boldsymbol{y}}(k)(k = 1, \dots, N)$ is defined as follows:

$$\mathbf{Y} = \left[\underline{\boldsymbol{y}}(1) \cdots \underline{\boldsymbol{y}}(N)\right] \tag{2}$$

The linear BSS problem is defined as [18]:

$$\underline{\boldsymbol{y}}(k) = \mathbf{T}\underline{\boldsymbol{s}}(k) + \underline{\boldsymbol{\epsilon}}(k) \tag{3}$$

where $\mathbf{T}$ is the mixing matrix, $\underline{\boldsymbol{s}}(k) = \left[s_1(k) \ \dots s_{n_y}(k)\right]^T$ is the sources vector and $\underline{\boldsymbol{\epsilon}}(k) = \left[\epsilon_1(k) \ \dots \epsilon_{n_y}(k)\right]^{\mathrm{T}}$ represents all the uncertainties and perturbation effects (modeling uncertainty and noises). In our study, we will consider the noise-free model (4), dealing with uncertainties and perturbations will be done by generating a robust bound for detection decision:

$$\underline{\boldsymbol{y}}(k) = \mathbf{T}\underline{\boldsymbol{s}}(\mathrm{k}) \tag{4}$$

BSS is an estimation problem, and it is accomplished by finding simultaneously an estimated sources vector $\underline{\hat{\boldsymbol{s}}}(k)$ and a separation matrix noted $\mathbf{W}$ only from the observed data $\underline{\boldsymbol{y}}(k)$:

$$\underline{\boldsymbol{r}}(k) = \underline{\hat{\mathbf{s}}}(k) = \mathbf{W}\underline{\boldsymbol{y}}(k) \tag{5}$$

where $\underline{\boldsymbol{r}}(k) = \left[r_1 \cdots r_{n_y}\right]^T \in \mathbb{R}^{n_y \times 1}$ and $\mathbf{W} \in \mathbb{R}^{n_y \times n_y}$ are respectively the estimated sources vector at instant k and the separation matrix. Equation (5) is called the separation model.

Clearly, without additional assumptions, the BSS problem (equation (5)) is ill-posed. Cardoso [22] has shown that the BSS problem can be resolved using assumptions done on the nature of sources. In this paper, we assume that the sources are temporally identically and

independently distributed (*iid*) and Gaussian, which leads to the principal component analysis method.

2.2. *Principal component analysis*

The separation of sources relies on the basic knowledge of the mutual independence of source components. It is then natural to resolve the BSS problem by minimizing a dependence criterion between these components. In our study, we adopt the mutual information as the separation criterion [23]. From equation (5), the solution is to find the matrix **W**, so that the mutual information is zero. In the case where the sources are assumed to follow Gaussian distribution, the mutual information $I(\underline{\boldsymbol{r}})$ is given by [24]:

$$I(\underline{\boldsymbol{r}}) = \frac{1}{2}\ln\frac{\prod_{i=1}^{n_y}\sigma_{r_i}^2}{\det(\boldsymbol{\Sigma}_{\underline{\boldsymbol{r}}})} \tag{6}$$

If the components r_i of the vector $\underline{\boldsymbol{r}}$ have to be statistically independent, mutual information defined in (6) is equivalent to:

$$I(\underline{\boldsymbol{r}}) = 0 \quad \Rightarrow \quad \prod_{i=1}^{n_y}\sigma_{r_i}^2 = \det(\boldsymbol{\Sigma}_{\underline{\boldsymbol{r}}}) \tag{7}$$

Knowing that covariance matrix $\boldsymbol{\Sigma}_{\underline{\boldsymbol{r}}}$ is symmetric, equality (7) is satisfied if the covariance matrix $\boldsymbol{\Sigma}_{\underline{\boldsymbol{r}}}$ is diagonal: the sources are uncorrelated and statistically independent [16]. Principal component analysis of a measurement vector $\underline{\boldsymbol{y}}$ is defined as a pair of matrices $\left\{\mathbf{P}, \boldsymbol{\Lambda}_{\boldsymbol{\Sigma}_{\underline{\boldsymbol{y}}}}\right\}$ such that the covariance matrix $\boldsymbol{\Sigma}_{\underline{\boldsymbol{y}}}$ is factorized:

$$\boldsymbol{\Sigma}_{\underline{\boldsymbol{y}}} = \mathbf{P}\boldsymbol{\Lambda}_{\boldsymbol{\Sigma}_{\underline{\boldsymbol{y}}}}\mathbf{P}^T \tag{8}$$

where $\mathbf{P} = \left[\underline{\boldsymbol{p}}_1 \cdots \underline{\boldsymbol{p}}_{n_y}\right] \in \mathbb{R}^{n_y \times n_y}$ is the matrix of eigenvectors and is a diagonal matrix of eigenvalues.

The separation matrix, noted now $\mathbf{W}_{\text{PCA}}$, is given by:

$$\mathbf{W}_{\text{PCA}} = \boldsymbol{\Lambda}_{\boldsymbol{\Sigma}_{\underline{\boldsymbol{y}}}}^{-\frac{1}{2}}\mathbf{P}^T \tag{9}$$

In order to reduce the number of principal components, we use the cumulative percent variance CPV [25]. It is a measure of the percent variance captured by the first n_r PCs:

$$\text{CPV}(n_r) = 100\frac{\sum_{i=1}^{n_r}\lambda_i}{\sum_{i=1}^{n_y}\lambda_i} \tag{10}$$

3. *Damage detection procedure*

3.1. *Feature extraction*

We seek to detect changes in the structure by monitoring specific features estimated from baseline observation set (referred by the exponent "s") and observation set of a current or unknown state (referred by the exponent "u"). We note $\mathbf{Y}^s$, $\mathbf{Y}^u$, respectively, the measurement matrix of the structure in a healthy and unknown state.

To define the feature, we use the separation matrices $\mathbf{W}_{\mathrm{PCA}}^s$ and $\mathbf{W}_{\mathrm{PCA}}^u$. From (9), we have:

$$\mathbf{W}_{\mathrm{PCA}}^s = \boldsymbol{\Lambda}_{\boldsymbol{\Sigma}_{\underline{y}^s}}{}^{-\frac{1}{2}}(\mathbf{P}^s)^T \tag{11}$$

$$\mathbf{W}_{\mathrm{PCA}}^u = \boldsymbol{\Lambda}_{\boldsymbol{\Sigma}_{\underline{y}^u}}{}^{-\frac{1}{2}}(\mathbf{P}^u)^T \tag{12}$$

If the reduction using a fixed CPV is possible (see subsection 2.2), the separating matrix $\mathbf{W}_{\mathrm{PCA}}^s$ and $\mathbf{W}_{\mathrm{PCA}}^u$ are rewritten as follows:

$$\begin{aligned}\mathbf{W}_{\mathrm{PCA}}^s &= \mathbf{I}_{n_y\times n_y}\boldsymbol{\Gamma}^s(\mathbf{V}^s)^T = \begin{bmatrix}\mathbf{I}_{n_y\times n_r} & \mathbf{I}_{n_y\times(n_y-n_r)}\end{bmatrix}\begin{bmatrix}\boldsymbol{\Gamma}_1^s & \mathbf{0}\\ \mathbf{0} & \boldsymbol{\Gamma}_2^s\end{bmatrix}\begin{bmatrix}\mathbf{V}_1^s & \mathbf{V}_2^s\end{bmatrix}^T\\ &= \mathbf{W}_{\mathrm{PCA1}}^s + \mathbf{W}_{\mathrm{PCA2}}^s\end{aligned} \tag{13}$$

where:

$\boldsymbol{\Gamma}_1^s = \mathrm{diag}\left(\sigma_1 \cdots \sigma_{n_r}\right)$, $\mathbf{V}_1^s = \left[\underline{\boldsymbol{v}}_{11}^s \cdots \underline{\boldsymbol{v}}_{1n_r}^s\right] \in \mathbb{R}^{n_y\times n_r}$ and $\mathbf{W}_{\mathrm{PCA1}}^s \in \mathbb{R}^{n_y\times n_y}$ are respectively the matrix of singular values, the matrix of right singular vectors and the separation matrix associated to the principal subspace of the healthy structure.

$\boldsymbol{\Gamma}_2^s = \mathrm{diag}\left(\sigma_{n_r+1} \cdots \sigma_{n_y}\right)$, $\mathbf{V}_2^s = \left[\underline{\boldsymbol{v}}_{2(n_r+1)}^s \cdots \underline{\boldsymbol{v}}_{2n_y}^s\right] \in \mathbb{R}^{n_y\times(n_y-n_r)}$ and $\mathbf{W}_{\mathrm{PCA2}}^s \in \mathbb{R}^{n_y\times n_y}$ are respectively the matrix of singular values, the matrix of right singular vectors and the separation matrix associated to the residual subspace of the healthy structure.

In the same way, we define the matrix $\mathbf{W}_{\mathrm{PCA}}^u$ using the following equation:

$$\begin{aligned}\mathbf{W}_{\mathrm{PCA}}^u &= \mathbf{I}_{n_y\times n_y}\boldsymbol{\Gamma}^u(\mathbf{V}^u)^T = \begin{bmatrix}\mathbf{I}_{n_y\times n_r} & \mathbf{I}_{n_y\times(n_y-n_r)}\end{bmatrix}\begin{bmatrix}\boldsymbol{\Gamma}_1^u & \mathbf{0}\\ \mathbf{0} & \boldsymbol{\Gamma}_2^u\end{bmatrix}\begin{bmatrix}\mathbf{V}_1^u & \mathbf{V}_2^u\end{bmatrix}^T\\ &= \mathbf{W}_{\mathrm{PCA1}}^u + \mathbf{W}_{\mathrm{PCA2}}^u\end{aligned} \tag{14}$$

The presence of a damage will modify the measurement matrix $\mathbf{Y}^s$, and consequently the separation matrix $\mathbf{W}_{\mathrm{PCA}}^u$, compared to the matrix $\mathbf{W}_{\mathrm{PCA}}^s$. Therefore, the subspaces generated by $\mathbf{W}_{\mathrm{PCA}}^u$ are deflected to those of $\mathbf{W}_{\mathrm{PCA}}^s$. The idea here is to monitor changes of specific subspaces.

Let, $R\{\mathbf{A}\}$, $R\{\mathbf{A}^T\}$ be respectively the range subspace of a matrix $\mathbf{A} \in \mathbb{R}^{n_y \times n_y}$ and its transpose. $\mathbf{P}_{R\{\mathbf{A}\}}$, $\mathbf{P}_{R\{\mathbf{A}^T\}}$ correspond to the orthogonal projection of the range subspace $R\{\mathbf{A}\}$ and $R\{\mathbf{A}^T\}$. One way to define orthogonal projections is to use SVD, *i.e.*

$$\mathbf{\Gamma} = \mathbf{U}^T \mathbf{A} \mathbf{V} = \text{diag}\left(\sigma_1 \cdots \sigma_{n_y}\right) \tag{15}$$

The orthogonal projections $\mathbf{P}_{R\{\mathbf{A}\}}$, $\mathbf{P}_{R\{\mathbf{A}^T\}}$ are respectively defined as follow [26]:

$$\mathbf{P}_{R\{\mathbf{A}\}} = \mathbf{U}\mathbf{U}^T \ , \mathbf{P}_{R\{\mathbf{A}^T\}} = \mathbf{V}\mathbf{V}^T \tag{16}$$

From the definition of the separating matrices $\mathbf{W}_{\text{PCA}}^s$ and $\mathbf{W}_{\text{PCA}}^u$, the matrix of left singular vectors is equal to the identity matrix:

$$\mathbf{U}^s = \mathbf{U}^u = \mathbf{I}_{n_y} \tag{17}$$

Therefore, no information can be derived from the matrix of left singular vectors, thus we will use the matrix of right singular vectors as a feature. To build our proposed damage index, we will use projections on the transpose of matrices $\mathbf{W}_{\text{PCA1}}^s$ and $\mathbf{W}_{\text{PCA1}}^u$ as a damage feature. This is the subject of the following subsection.

3.2. *Damage index*

Following the work of [14], the proposed damage index is constructed using the calculation of the principal angle vectors between the range subspace of the matrix $(\mathbf{W}_{\text{PCA1}}^s)^T$ and $(\mathbf{W}_{\text{PCA1}}^u)^T$.

We note $\underline{\boldsymbol{\varphi}}[R\{(\mathbf{W}_{\text{PCA1}}^u)^T\}, R\{(\mathbf{W}_{\text{PCA1}}^s)^T\}]$, the principal angle vectors between the range subspace $R\{(\mathbf{W}_{\text{PCA1}}^u)^T\}$ and $R\{(\mathbf{W}_{\text{PCA1}}^s)^T\}$. Using the SVD tool, the Euclidean norm of the sinus angle of these vectors is defined as follow [27]:

$$\begin{aligned} \left\| \sin \underline{\boldsymbol{\varphi}}[R\{(\mathbf{W}_{\text{PCA1}}^u)^{\text{T}}\}, R\{(\mathbf{W}_{\text{PCA1}}^s)^{\text{T}}\}] \right\|_2 &= \left\| \mathbf{P}_{R\left\{(\mathbf{W}_{\text{PCA1}}^s)^{\text{T}}\right\}^{\perp}} \mathbf{P}_{R\left\{(\mathbf{W}_{\text{PCA1}}^u)^{\text{T}}\right\}} \right\|_2 \\ &= \left\| \left(\mathbf{I}_{n_r} - \mathbf{P}_{R\left\{(\mathbf{W}_{\text{PCA1}}^s)^T\right\}}\right) \mathbf{P}_{R\left\{(\mathbf{W}_{\text{PCA1}}^u)^T\right\}} \right\|_2 \end{aligned} \tag{18}$$

In [14], the principal angle vectors are calculated using the QR decomposition and the cosines of the principal angles. Their damage index is given by the largest angle. Here, we propose the following damage index:

Proposal 1: Damage index

Let be a smart structure with n_y sensors, and define equations (13), (14) *and* (18). *Damage could be detected by monitoring the following damage index:*

$$\mathrm{DI}_{\mathrm{PCA}} = \frac{\left\| \sin \underline{\boldsymbol{\varphi}}[R\{(\mathbf{W}_{\mathrm{PCA1}}^{u})^{T}\}, R\{(\mathbf{W}_{\mathrm{PCA1}}^{s})^{T}\}] \right\|_{2}}{n_r} \tag{19}$$

where n_r is the number of principal components retained.

In the absence of disturbances and when the structure at an unknown state is healthy, the damage index $\mathrm{DI}_{\mathrm{PCA}}$ is zero. Otherwise, the structure is damaged. However, as the measurements are corrupted by noises and unknown perturbations, the detection decision could be biased. Moreover, these perturbations might also affect the distinguishability between damage and environmental disturbances and consequently the isolationability of damages. To deal with this problem, we propose using matrix perturbation theory, to calculate an analytical upper bound of these small perturbations. This is the aim of the next subsection.

3.3. *Analytic threshold*

As stated previously, the proposed damage index is based on subspace projections and decompositions. Due to various perturbation sources such as finite data effect, measurement noises and temperature change, perturbations arise in subspaces. Therefore, false alarms could appear.

To handle these perturbations, we propose to use matrix perturbation analysis that can result in defining an analytical bound with no rely of statistical assumptions usually performed for damage detection. Matrix perturbation theory considers how matrix functions such as subspaces change when the matrix is subject to perturbations.

In this work, we consider that separation matrix obtained from the baseline, is slightly perturbed, *i.e.*

$$\widetilde{\mathbf{W}}_{\mathrm{PCA}}^{s} = \mathbf{W}_{\mathrm{PCA}}^{s} + \delta\mathbf{W}_{\mathrm{PCA}}^{s} \tag{20}$$

where $\widetilde{\mathbf{W}}_{\mathrm{PCA}}^{s}$ is a perturbed version of $\mathbf{W}_{\mathrm{PCA}}^{s}$ with perturbation $\delta\mathbf{W}_{\mathrm{PCA}}^{s}$.

Then, we propose to define a robustness measure that estimates how much the damage index (defined in (19)) is affected. The overtaking of this rigorous threshold will indicate the presence of damage. It will also minimize false-positive and false-negative alarms.

To drive the proposed analytical bound, we use early work of Wedin [28] on perturbed matrices in connection with SVD. The idea is to estimate $\|\delta\mathbf{W}_{\mathrm{PCA}}^{s}\|$ by performing several tests or simulations on the healthy structure and to evaluate the gap between specific singular values in order to find an upper bound for $\mathrm{DI}_{\mathrm{PCA}}$. Background materials on matrix perturbation theory and Wedin framework results can be provided in [21;26]. It is to be noted that our approach is an unsupervised learning mode (ULM), which implies that data from a damaged state are not used to build this bound. This ULM is mandatory necessary for real-world application.

The proposed analytic bound is derived following three major steps:

First step: testing the healthy structure

Consider the variation $\delta\mathbf{W}_{\mathrm{PCA}}^{s}$ that the separation matrix $\mathbf{W}_{\mathrm{PCA}}^{s}$ is subject due to the environmental disturbances. To describe this variation $\delta\mathbf{W}_{\mathrm{PCA}}^{s}$, we perform a **second** test on the healthy structure, we apply the PCA method and we determine the new separation matrix noted $\widetilde{\mathbf{W}}_{\mathrm{PCA}}^{s}$. The matrix $\delta\mathbf{W}_{\mathrm{PCA}}^{s}$ is defined by the following relationship:

$$\widetilde{\mathbf{W}}_{\mathrm{PCA}}^{s} = \mathbf{W}_{\mathrm{PCA}}^{s} + \delta\mathbf{W}_{\mathrm{PCA}}^{s} \tag{21}$$

The SVD of the matrix $\widetilde{\mathbf{W}}_{\mathrm{PCA}}^{s}$ is given by:

$$\widetilde{\mathbf{W}}_{\mathrm{PCA}}^{s} = \begin{bmatrix}\mathbf{I}_{n_y\times n_r} & \mathbf{I}_{n_y\times(n_y-n_r)}\end{bmatrix}\begin{bmatrix}\tilde{\mathbf{\Gamma}}_1^{s} & \mathbf{0}\\ \mathbf{0} & \tilde{\mathbf{\Gamma}}_2^{s}\end{bmatrix}[\widetilde{\mathbf{V}}_1^{s} \quad \widetilde{\mathbf{V}}_2^{s}]^T = \widetilde{\mathbf{W}}_{\mathrm{PCA1}}^{s} + \widetilde{\mathbf{W}}_{\mathrm{PCA2}}^{s} \tag{22}$$

We first define the following residual matrices and norms:

$$\mathbf{R}_{11} = \mathbf{W}_{\mathrm{PCA}}^{s}\widetilde{\mathbf{V}}_1^{s} - \widetilde{\mathbf{U}}_1^{s}\tilde{\mathbf{\Gamma}}_1^{s} = \mathbf{W}_{\mathrm{PCA}}^{s}\widetilde{\mathbf{V}}_1^{s} - \widetilde{\mathbf{U}}_1^{s}\left[\left(\widetilde{\mathbf{U}}_1^{s}\right)^T\widetilde{\mathbf{W}}_{\mathrm{PCA}}^{s}\widetilde{\mathbf{V}}_1^{s}\right] = -\delta\mathbf{W}_{\mathrm{PCA}}^{s}\widetilde{\mathbf{V}}_1^{s} \tag{23}$$

$$\mathbf{R}_{21} = (\mathbf{W}_{\mathrm{PCA}}^{s})^T\widetilde{\mathbf{U}}_1^{s} - \widetilde{\mathbf{V}}_1^{s}\left(\tilde{\mathbf{\Gamma}}_1^{s}\right)^T = -(\delta\mathbf{W}_{\mathrm{PCA}}^{s})^T\widetilde{\mathbf{U}}_1^{s} = -(\delta\mathbf{W}_{\mathrm{PCA}}^{s})^T \tag{24}$$

And then evaluate their two norm, *i.e.*:

$$\|\mathbf{R}_{11}\|_2 = \left\|\delta\mathbf{W}_{\mathrm{PCA}}^{s}\widetilde{\mathbf{V}}_1^{s}\right\|_2 = \left\|\delta\mathbf{W}_{\mathrm{PCA}}^{s}\mathbf{P}_{R\left\{\left(\widetilde{\mathbf{W}}_{\mathrm{PCA1}}^{s}\right)^{\mathrm{T}}\right\}}\right\|_2 \tag{25}$$

$$\|\mathbf{R}_{21}\|_2 = \left\|(\delta\mathbf{W}_{\mathrm{PCA}}^{s})^T\mathbf{I}_{n_y\times n_r}\right\| = \left\|\mathbf{P}_{R\{\widetilde{\mathbf{W}}_{\mathrm{PCA1}}^{s}\}}\delta\mathbf{W}_{\mathrm{PCA}}^{s}\right\|_2 \tag{26}$$

where $\mathbf{P}_{R\{\widetilde{\mathbf{W}}_{\mathrm{PCA1}}^{s}\}}$ and $\mathbf{P}_{R\left\{\left(\widetilde{\mathbf{W}}_{\mathrm{PCA1}}^{s}\right)^{T}\right\}}$ are respectively the orthogonal projection of the matrix $\widetilde{\mathbf{W}}_{\mathrm{PCA1}}^{s}$ and its transpose.

From these relations, we introduce the number ε:

$$\varepsilon = \max(\|\mathbf{R}_{11}\|_2, \|\mathbf{R}_{21}\|_2) \tag{27}$$

This number quantifies the magnitude of the environmental disturbances.

We are now going to matrix perturbation theory through the work of Wedin and its principal results.

Second step: Matrix perturbation theory [28]

Our aim is to find an analytic upper bound to $\mathrm{DI}_{\mathrm{PCA}}$ (see (19)). Consequently, when we have estimates $\|\delta\mathbf{W}_{\mathrm{PCA}}^{s}\|$ and the gap between the least singular value of $\widetilde{\mathbf{W}}_{\mathrm{PCA1}}^{s}$ and the largest singular value of $\mathbf{W}_{\mathrm{PCA2}}^{s}$.

Assume now, that $\exists\, \eta \geq 0 \; and \; \delta > 0$, such that :

$$\eta \leq \sigma_{\max}(\mathbf{W}_{\mathrm{PCA2}}^{s}) = \|\mathbf{W}_{\mathrm{PCA2}}^{s}\|_2 \tag{28}$$

$$\eta + \delta \leq \sigma_{\min}\left(\widetilde{\mathbf{W}}_{\mathrm{PCA1}}^{s}\right) = \frac{1}{\left\|\widetilde{\mathbf{W}}_{\mathrm{PCA1}}^{s}{}^{-1}\right\|_2} \tag{29}$$

So:

$$\widetilde{\mathrm{DI}}_{\mathrm{PCA}}^{1} = \left\|\sin \underline{\boldsymbol{\theta}}\left[R\{\widetilde{\mathbf{W}}_{\mathrm{PCA1}}^{s}\}, R\{\mathbf{W}_{\mathrm{PCA1}}^{s}\}\right]\right\|_2 \leq \frac{\varepsilon + \eta\widetilde{\mathrm{DI}}_{\mathrm{PCA}}^{2}}{\eta + \delta} \tag{30}$$

$$\widetilde{\mathrm{DI}}_{\mathrm{PCA}}^{2} = \left\|\sin \underline{\boldsymbol{\varphi}}\left[R\left\{\left(\widetilde{\mathbf{W}}_{\mathrm{PCA1}}^{s}\right)^{T}\right\}, R\{(\mathbf{W}_{\mathrm{PCA1}}^{s})^{T}\}\right]\right\|_2 \leq \frac{\varepsilon + \eta\widetilde{\mathrm{DI}}_{\mathrm{PCA}}^{1}}{\eta + \delta} \tag{31}$$

Third step: elaboration of the bound

Recall that the damage index $\mathrm{DI}_{\mathrm{PCA}}$ (see (19)) is calculated from the separation matrix $\mathbf{W}_{\mathrm{PCA1}}^{s}$ of the healthy state and $\mathbf{W}_{\mathrm{PCA1}}^{u}$ of the structure in an unknown state, while the term $\widetilde{\mathrm{DI}}_{\mathrm{PCA}}^{2}$ is calculated from the separation matrix $\mathbf{W}_{\mathrm{PCA1}}^{s}$and $\widetilde{\mathbf{W}}_{\mathrm{PCA1}}^{s}$ from a second healthy test.

As the matrix of singular vectors of separation matrices equals the identity matrix, the term $\widetilde{\mathrm{DI}}_{\mathrm{PCA}}^{1} = 0$. Consequently, the term $\widetilde{\mathrm{DI}}_{\mathrm{PCA}}^{2}$ satisfies:

$$\widetilde{\mathrm{DI}}_{\mathrm{PCA}}^{2} \leq \frac{\varepsilon}{\eta + \delta} \tag{32}$$

Proposal 2*: *Analytic bound

The proposed bound is defined as follow:

$$\beta_{\mathrm{PCA}} = \gamma \frac{\varepsilon}{(\eta + \delta)n_r} \tag{33}$$

where:

ε *quantifies the magnitude of the environmental disturbances and it is defined in* (27),

η *and* δ *are defined respectively in* (28) *and* (29),

n_r *is the number of principal components retained,*

$\gamma \geq 1$ *is a tuning parameter adjusting the bound.*

The proof of this proposal is sketched in [29] and is quite straightforward, from results in [28].

Our proposed damage index and its associated bound are quantified numerically, so we can calculate a detection rate $\mathrm{R_{PCA}}$, which is defined as follow:

$$\mathrm{R_{PCA}} = \frac{\mathrm{DI_{PCA}}}{\beta_{\mathrm{PCA}}} \tag{34}$$

if $\mathrm{R_{PCA}} > 1$ then the structure is damaged, otherwise it is healthy.

3.4. *Framework of the damage detection procedure*

For practical implementation, we outline in this subsection the following framework. We assume that the measurements have been scaled (zero mean and unity variance).

Step 1: ***Tests of the healthy structure state***

1.1 *Make a first test of the healthy structure,*

1.2 *Make n other tests of the healthy structure with enough time lag between tests,*

1.3. *Build the measurement matrix* $\mathbf{Y}_0^s$ *of the healthy structure,*

1.4. *Build the n measurement matrices* $\widetilde{\mathbf{Y}}_i^s, i = 1 \ldots n$ *of the healthy structure.*

Step 2: ***Test of the structure at unknown state***

2.1. *Make one test of the structure at unknown state,*

2.2. *Build the measurement matrix* $\mathbf{Y}^u$ *of the structure at unknown state.*

Step 3: ***Calculate the damage index*** $\mathrm{DI_{PCA}}$

3.1. *Apply PCA to the measurement matrix* $\mathbf{Y}_0^s$,

3.2. *Calculate the separating matrix* $\mathbf{W}_{\mathrm{PCA}}^s$ *following equation* (11),

3.3. *Apply SVD to the* $\mathbf{W}_{\mathrm{PCA}}^s$ *following equation* (13),

3.4. *Calculate the separating matrix* $\mathbf{W}_{\mathrm{PCA}}^u$ *following equation* (12),

3.5. *Apply SVD to the* $\mathbf{W}_{\mathrm{PCA}}^u$ *following equation* (14),

3.6. *Calculate the damage index* $\mathrm{DI_{PCA}}$ *following the proposal 1* (see equation (19)).

Step 4: ***Calculate the bound*** $\mu_{\mathcal{B},\mathrm{PCA}}$ ***associated to the damage index*** $\mathrm{DI_{PCA}}$

4.1. *Take back the result of step 3.2, and repeat for i=1 to n the following steps:*

4.1.1. *Calculate the separating matrix* $\left(\widetilde{\mathbf{W}}_{\mathrm{PCA}}^{s}\right)^{i}$, $i = 1 \ldots n$, *following* (11),

4.1.2. *Apply SVD to the matrix* $\widetilde{\mathbf{W}}_{\mathrm{PCA}}^{s}{}^{i}$ *following equation* (13),

4.1.3. *Calculate the variation* $\delta(\mathbf{W}_{\mathrm{PCA}}^{s})^{i}$*using the following equation:*

$$\delta\mathbf{W}_{\mathrm{PCA}}^{s} = \mathbf{W}_{\mathrm{PCA}}^{s} - \widetilde{\mathbf{W}}_{\mathrm{PCA}}^{s}{}^{i}$$

4.1.4. *Calculate the analytic bound* $\beta_{i,\mathrm{PCA}}$ *following* (33) (see *proposal 2*),

4.2. *Calculate the mean of the bound* $\mu_{\beta,\mathrm{PCA}}$:

$$\mu_{\beta,\mathrm{PCA}} = \frac{1}{n}\sum_{i=1}^{n}\beta_{i,\mathrm{PCA}}$$

Step 5: Decision-making

Check if $\mathrm{R}_{\mathrm{PCA}} > 1$. *If it is the case, then the structure is damaged, otherwise it is healthy.*

4. *Example through FE simulations*

Before applying our damage detection methodology on a conformal load-bearing antenna structure (CLAS), we have first applied it through a finite element (FE) model of a composite plate.

Consider a rectangular carbone epoxy plate with dimensions $(400 \times 300 \times 2\ \mathrm{mm}^3)$ and made up of 16 layers. The layer sequences are: $(0°_2, 45°_2, -45°_2, 90°_2, 90°_2, -45°_2, 45°_2, 0°_2)$ and the mechanical properties of the composite material in nominal conditions are illustrated in table 1. In our case, nominal condition means that effects of temperature change are not taken into account. Using the controllability and observability gramians, we have performed in a previous work [30], an optimal placement of piezoceramic patches with dimensions $(30 \times 20 \times 0.2\ \mathrm{mm}^3)$. These piezoceramic patches belong to the PZ 29 family, table 2 depicts the mechanical and electrical properties of these PZT. The FE model of the composite plate equipped with its piezoceramics was developed using Structural Dynamic toolbox [31]. We have chosen a model with 195 elements, each element has dimension of $15 \times 10\ \mathrm{mm}^2$. The plate is under free-free boundary conditions. Figure 2 shows the composite plate model with the optimal placement of the PZT.

To apply the damage detection methodology described in subsection 3.4, we have first built the baseline of the healthy plate model in nominal conditions (see table 1). For this purpose, we have used PZT 7 as an actuator, while the others PZT are sensors ($n_y = 8$), then the continuous state space of the model was calculated with $n_m = 50$ modes. The damping was assumed to be equal to 0.05% for all modes. Once the continuous state space calculated, we have discretized it with sampling frequency $f_s = 100$ kHz. The excitation of actuator PZT 7

consists in a signal pulse with 1ms width, signal sensors were recorded with $N = 2^{16}$ time samples.

In section 2, we have stated that PCA can allow use to reduce the dimension of the measurement matrix. According to a fixed CPV of 98%, we have retained seven principal components ($n_r = 7$).

Table 1: Mechanical properties of the composite material

Property	E_1 (GPa)	$E_2 = E_3$ (GPa)	$G_{12} = G_{13}$ (GPa)	G_{23} (GPa)	$\nu_{12} = \nu_{12}$	ν_{23}	$\rho\ (Kg/m^3)$
Value	127.7	7.217	5.712	2.614	0.318	0.38	1546

Table 2: Mechanical and electrical properties of the PZ29 [32]

Property	E (GPa)	ν	ρ (Kg/m^3)	d_{31}(C/N)	d_{33} (C/N)	Curie temperature C°
Value	58.8	0.3	7460	-2.43×10^{-10}	5.74×10^{-10}	235

4.1. *Perturbation by measurement noises*

We have first simulated the effect of environmental perturbations as a noise disturbance acting on the dynamic response data:

56 simulations were achieved using the composite plate model in different conditions of measurement noises. Table 3 summarizes these simulations. The first reflects the composite model in a healthy state with 0.25% variance noise of the energy contained in the simulated data sensors, simulations n°2 to 50 correspond to the healthy state, but with different values of noise variance (from 0.26% to 0.75% with a step of 0.01%). These simulations will allow us to build the analytic bound $\mu_{\beta,PCA}$. It is to be noted, that in the nominal conditions, the value of coefficient γ defined in proposal 2 (see relation (33)) is equal to 1.

Simulations 51-55 correspond to damaged states of the composite plate model. These simulations are associated respectively to a reduced stiffness of 5% for element 17, 56, 140, 37 and 184 (see figure 2), with a variance noise of 0.5%. Figure 3 depicts the time response of sensor PZT 1 for simulations n°1 (healthy state) and n°56 (damaged state: reduced stiffness of 5% for the element 17), only the 512 first samples are displayed.

Table 4 depicts the results of the damage detection through these simulations. One can see that for the damaged states, the associated damage index DI_{PCA} is upper than the proposed bound $\mu_{\beta,PCA}$, so the damaged states are well detected. Figure 4 is a visualization manner for the decision making.

Table 3: Simulation states for the composite plate model

Simulation n°	State
1-50	Healthy state: used to build the analytic bound
51	Damaged 1: Reduced stiffness of 5% for the element 17
52	Damaged 2: Reduced stiffness of 5% for the element 56:
53	Damaged 3: Reduced stiffness of 5% for the element 140
54	Damaged 4: Reduced stiffness of 5% for the element 37
55	Damaged 5: Reduced stiffness of 5% for the element 184

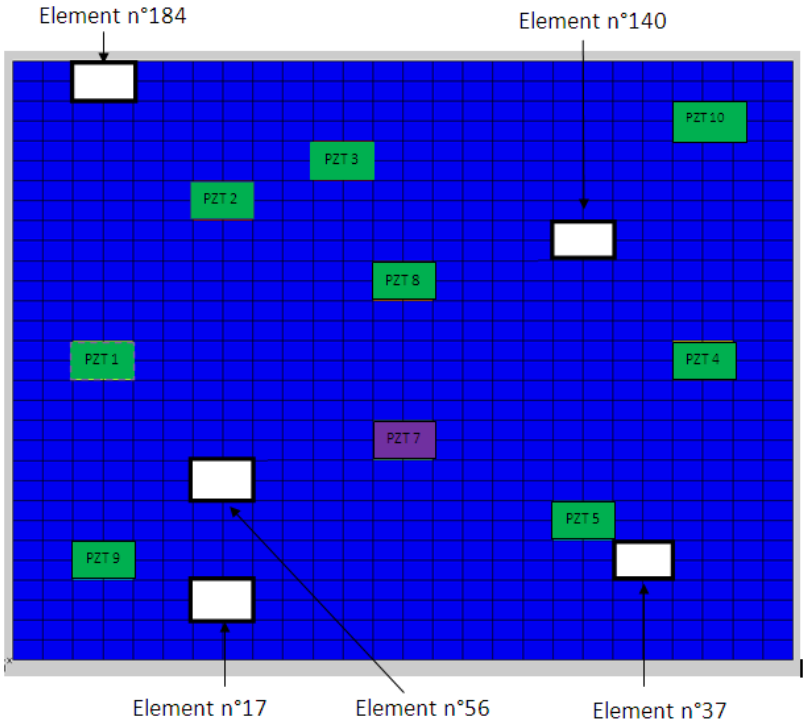

Figure 2: Finite element model of a composite plate bounded with piezoceramic patches

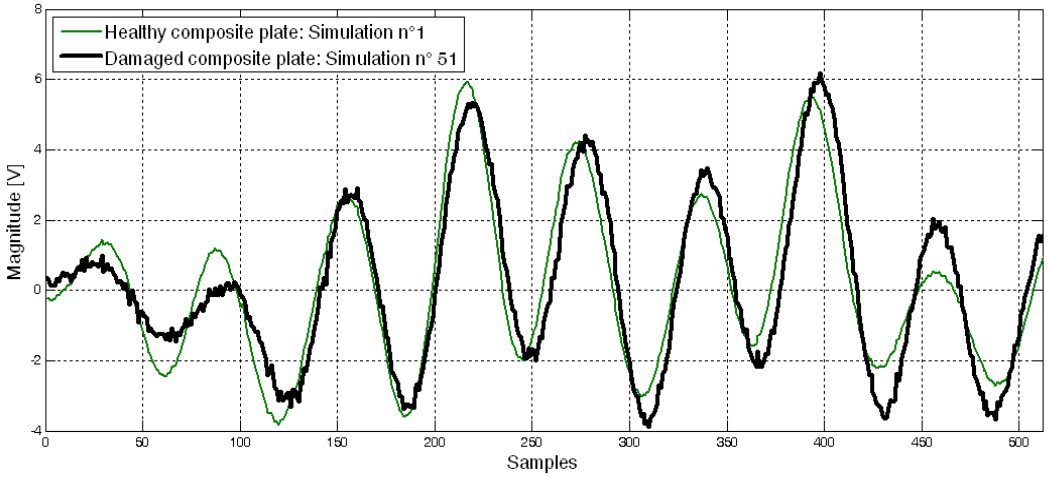

Figure 3: Impulse response of the healthy and damaged structure: composite plate model

Table 4: Damage detection using the analytic bound: finite element model of a composite plate

Simulation n°	DI_{PCA}	$\mu_{\mathcal{B},PCA}$	$R_{PCA} = \frac{DI_{PCA}}{\mu_{\mathcal{B},PCA}}$	Decision
51	0.1532	0.0328	4.6707	Damaged
52	0.2000	0.0328	6.0976	Damaged
53	0.2887	0.0328	8.8018	Damaged
54	0.2248	0.0328	6.8537	Damaged
55	0.1936	0.0328	5.9024	Damaged

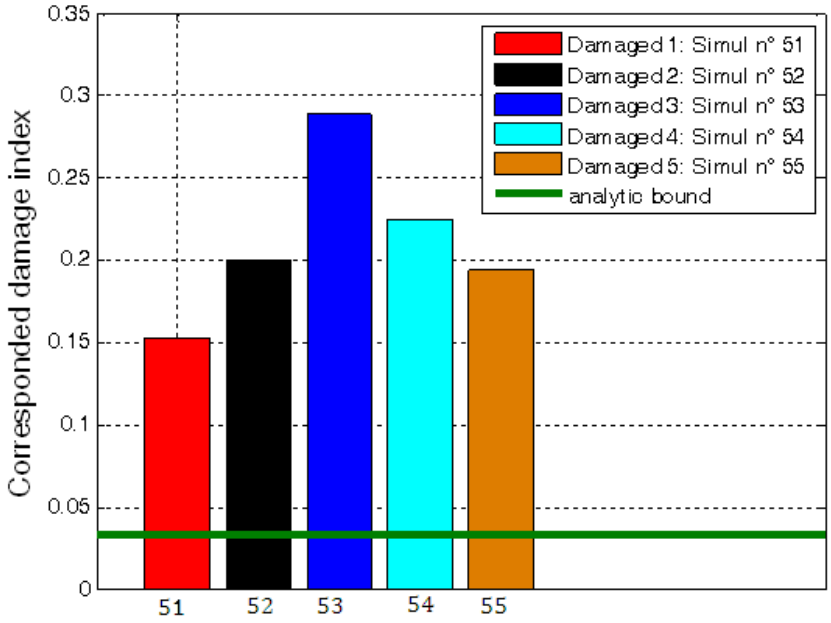

Figure 4: Visualization manner of the damage decision: composite plate model

4.2. *Perturbation by temperature change*

The main of this subsection is to study through the FE model, the effect of temperature in the decision making regarding alarm false.

With the inherent anisotropy of composite materials, any attempt to simulate the effect of environmental factors like temperature requires relevant experimental data from the structure in an enclosed heated space. These data will feed the FE model to yield reasonably accurate prediction. However, it is expected that first order thermal effects in an instrumented composite will be associated with the difference between the evolution of constitutive behavior of the composite matrix, its fibers and the piezoelectric. As a rough approximation, one can consider varying moduli for the composite plate with fixed mechanical properties for the piezoelectric material.

In order to mimic the temperature effects, we have modified the moduli $(E_1, E_2, G_{12}, G_{23})$ by a percentage $\alpha \in [0.01 \quad 0.014]$ %. Table 5 presents the basis of the modification under certain temperature change. According to this rough approximation, simulations were achieved. It is to be noted that for each simulation, 0.25% variance noise measurement was

added to each dynamic response. The damage indices associated to these simulations are depicted in table 6.

Table 5: Value of the simulated temperature under the perturbation of the moduli $(\mathrm{E}_1, \mathrm{E}_2,\ \mathrm{G}_{12}, \mathrm{G}_{23}\ )$

Simulation n°	Simulated temperature T [°C]
56: $\alpha = 0.01\%$	26
57: $\alpha = 0.011\%$	27
58: $\alpha = 0.012\%$	28
59: $\alpha = 0.013\%$	29
60: $\alpha = 0.014\%$	30

Table 6: Effect of the temperature in the damage detection

Simulation n°	$\mathrm{DI}_{\mathrm{PCA}}$	$\mu_{\mathcal{B},PCA}$	$\mathrm{R}_{\mathrm{PCA}} = \frac{\mathrm{DI}_{\mathrm{PCA}}}{\mu_{\mathcal{B},PCA}}$	Decision
56: $\alpha = 0.01\%$	0.0545	0.0328	1.6616	false positive alarms
57: $\alpha = 0.011\%$	0.0346	0.0328	1.0549	false positive alarms
58: $\alpha = 0.012\%$	0.0870	0.0328	2.6524	false positive alarms
59: $\alpha = 0.013\%$	0.0577	0.0328	1.7591	false positive alarms
60: $\alpha = 0.014\%$	0.0539	0.0328	1.6433	false positive alarms

The results depicted in this above table show that the damage index is greater than the analytic bound. Knowing that these simulations concern a healthy model, false positive alarms (FPA) were detected. So, we have to deal with these FPA.

4.3. *Handling the effect of the temperature*

Our strategy to handle the effect of temperature was to adapt the value of the bound by a judicious choice of the coefficient γ, defined in (33).

Let, $\left(\widetilde{\mathbf{W}}_{\mathrm{PCA}}^{s}\right)^{k}$, $k = 56$ to 60, be the perturbed separation matrices, obtained respectively from simulation 56 to 60. Each of these matrices captures the temperature effect through their singular values. According to this reasoning, we define γ as:

$$\gamma = \max \sigma_{max}\left(\left(\widetilde{\mathbf{W}}_{\mathrm{PCA}}^{s}\right)^{k}\right),\ k = 56 \text{ to } 60 \tag{35}$$

In order to test this strategy, we have simulated the temperature effect for the healthy and damaged models. Table 7 summarizes the studying model states in this subsection.

Table 8 shows the value of the updated bound, and the damage index associated to the different conditions of the composite model (see table 7). One can see that for the damaged states, the associated damage index $\mathrm{DI}_{\mathrm{PCA}}$ is upper than updated bound $\mu_{\mathcal{B},PCA}$. Moreover, in the case of temperature effect of the healthy state model, the damage index is less than the bound, so the false positive alarms presented in table 6 were entirely removed. In order to

have visualization for the decision making, we have plotted in figure 5, the damage rate versus the simulation number (according to table 7); we can obverse that the healthy and damaged model states are well separated, even if the temperature is present in our modeling manner. According to these results, we can assure that if the temperature change belongs to a certain interval, no false positive alarms will be detected.

Table 7: Simulation sate of the composite plate model: temperature effect

Simulation n°	State of the composite model by taken into account of the temperature effect
61	Healthy state: α = 0.0105% and 0.75% variance noise
62	Healthy state: α = 0.0115% and 0.25% variance noise
63	Healthy state: α = 0.0125% and 0.25% variance noise
64	Healthy state: α = 0.0135% and 0.50% variance noise
65	Healthy state: α = 0.014% and 0.50% variance noise
66	Damaged 6: Reduced stiffness of 5% for the element 17, α = 0.014% and 0.25% variance noise
67	Damaged 7: Reduced stiffness of 5% for the element 56, α = 0.013% and 0.5% variance noise
68	Damaged 8: Reduced stiffness of 5% for the element 140, α = 0.0125% and 0.75% variance noise
69	Damaged 9: Reduced stiffness of 5% for the element 37, α = 0.0115% and 0.5% variance noise
70	Damaged 10: Reduced stiffness of 5% for the element 184, α = 0.014% and 0.75% variance noise

Table 8: Results of the damage detection by taken into account the temperature effect

Simulation n°	$\mathrm{DI}_{\mathrm{PCA}}$	$\mu_{\mathcal{B},PCA}$	$\mathrm{R}_{\mathrm{PCA}} = \frac{\mathrm{DI}_{\mathrm{PCA}}}{\mu_{\mathcal{B},PCA}}$	Decision
61	0.0869	0.1037	0.8380	Healthy
62	0.0846	0.1037	0.8158	Healthy
63	0.0937	0.1037	0.9036	Healthy
64	0.0717	0.1037	0.6914	Healthy
65	0.0542	0.1037	0.5227	Healthy
66	0.2078	0.1037	2.0039	Damaged
67	0.1943	0.1037	1.8737	Damaged
68	0.1223	0.1037	1.1794	Damaged
69	0.2097	0.1037	2.0222	Damaged
70	0.2131	0.1037	2.0550	Damaged

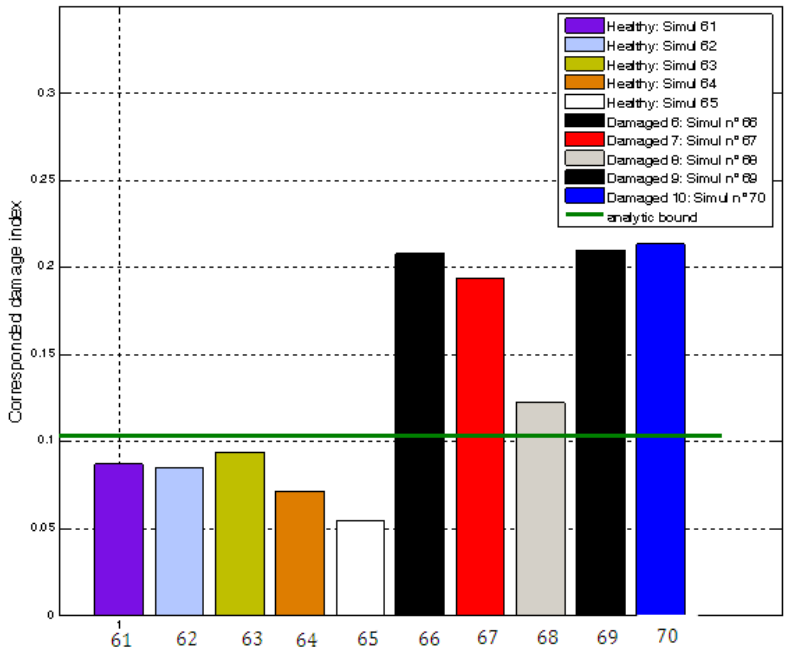

Figure 5: Results of handling the effect of temperature in a FE composite model

5. *Experimental test bench: Conformal load-bearing antenna structure*

The CLAS employed in this study consists of a piece of a composite fuselage. The dimension of this structure is $(800 \times 150 \times 2\text{mm}^3)$ and it is made up with the same layers as the composite plate model. The mechanical proprieties of the composite material are presented in table 1. Figure 6, 7 and 8 show respectively the antenna network of the CLAS, the seven PZT bonded on it (dimensions $(20 \times 30 \times 0.2\ \text{mm}^3)$, PZ29 family) and their locations.

Before applying the damage detection methodology, we have done simultaneously a radiation pattern and a measure of strain using the PZT sensors (figure 9) in order to check if there is coupling between the electromagnetic phenomena of the antenna network and the electrical information transmitted by the piezoelectric sensors. This study has shown that the two phenomena can coexist in the same time without any interaction.

The CLAS depicted in figure 8 was used first to build a baseline set. For that, we have used PZT 2 as an actuator, while the six others PZT are sensors ($n_y = 6$). The input excitation, and the data acquisition were done using a commercial system dSPACE®. This excitation consists in a signal pulse with 1ms width; signals were acquired with sampling frequency $f_s = 100$ kHz, and $N = 2^{16}$ time samples were recorded for each channel: one corresponding to the excitation applied to the PZT actuator, and the others concern the measurements collected by the PZT sensors. Several baseline tests with enough time lag between them were done on

the CLAS ($n = 14$) in order to calculate the analytic bound $\mu_{\beta,PCA}$. It is to be noted that these tests were done under temperature of T=18°C and T=24°C. In these conditions, the coefficient γ was set to one. Using a buckling device (figure 10), we have provoked in a second time a delamination of the antenna part from the host structure (figure 11).

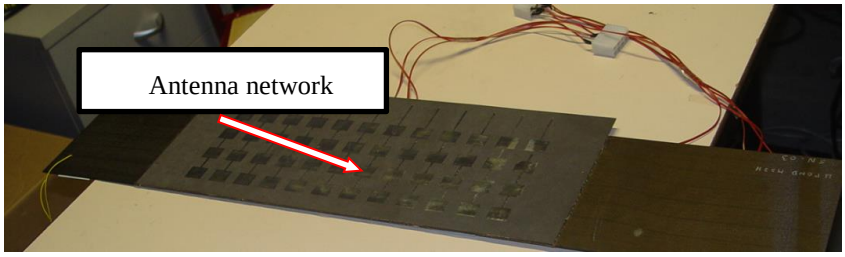

Figure 6: Antenna network of the CLAS

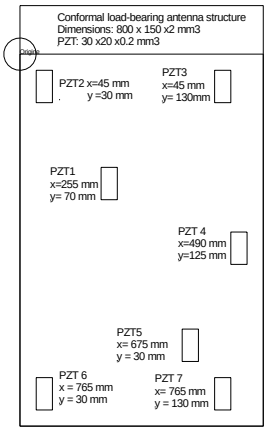

Figure 7: Location of the piezoceramic patches on the CLAS

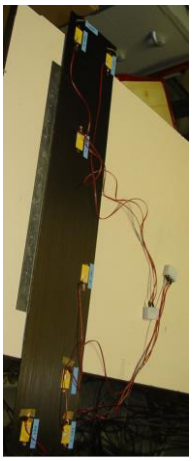

Figure 8: CLAS bounded with piezoceramic patches

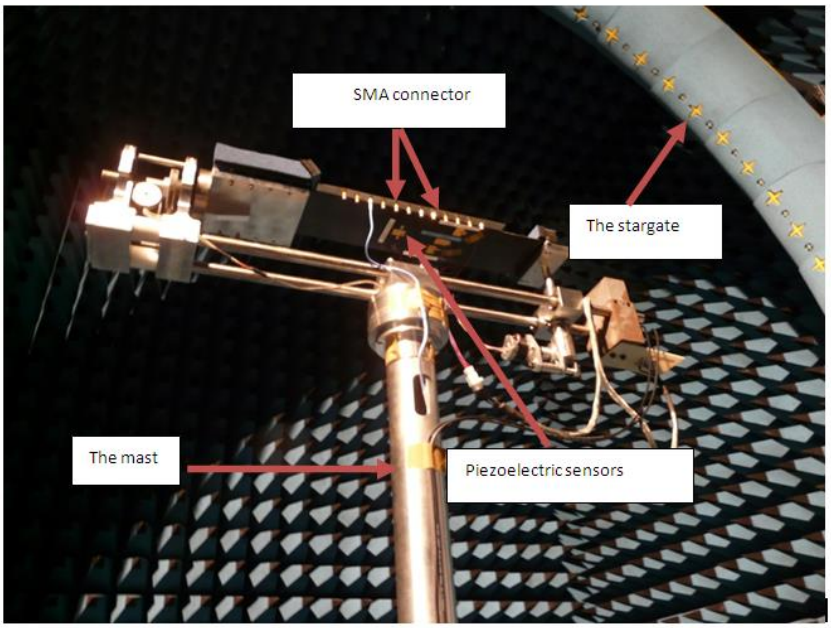

Figure 9: Test rig mounted in an anechoic chamber

Figure 10: Buckling device [5]

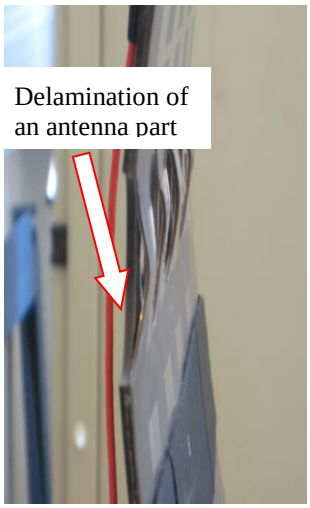

Figure 11: Delamination of an antenna part from the CLAS

6. *Application of the damage detection to the CLAS*

In this section, we proceed to the damage detection method within the framework of the CLAS. This method is governed by the damage index $\mathrm{DI}_{\mathrm{PCA}}$ (see proposal 1), and by the analytic bound (see proposal 2).

The damage detection methodology illustrated in subsection 3.4 was applied to the CLAS to detect two kinds of damage. The first concerns the detection of a hole (damage 1 with diameter of $27mm$) located at the middle of the CLAS (see figure 10), the second damage concerns a delamination of an antenna network part, and it is separated from the host structure by a distance of 22 mm (see figure 11). Let's begin by presenting the results of damage 1.

Damage detection result: damage 1

Table 9 depicts the result of our methodology to detect the hole of the CLAS. In this case, the damage index $\mathrm{DI}_{\mathrm{PCA}} = \mathbf{0.3159}$, and it is upper than the bound $\mu_{\beta,PCA} = \mathbf{0.0347}$. Moreover the damage rate $\mathrm{R}_{\mathrm{PCA}} = \frac{\mathrm{DI}_{\mathrm{PCA}}}{\mu_{\beta,\mathrm{PCA}}} = \mathbf{9.1037}$.

Table 9: Result of the damage detection of the CALS using PCA: damage 1

	$\mathrm{DI}_{\mathrm{PCA}}$	$\mu_{\beta,\mathrm{PCA}}$
Damage1 of the CLAS: hole	0.3159	0.0347

This result allows us to assert that the first damage was well detected. Now, we present the result of damage 2.

Damage detection result: damage 2

Once the damage 1 detected, we have provoked a delamination of an antenna network part from the CLAS (figure 11), we have done tests of this structure state and we have applied the damage detection procedure (the result is depicted in table 10). In this case, the damage index $\mathrm{DI}_{\mathrm{PCA}} = \mathbf{0.4292}$, and it is upper than the bound $\mu_{\beta,\mathrm{PCA}} = \mathbf{0.0347}$. Moreover the damage rate $\mathrm{R}_{\mathrm{PCA}} = \frac{\mathrm{DI}_{\mathrm{PCA}}}{\mu_{\beta,\mathrm{PCA}}} = \mathbf{12.3689}$. *Then damage 2 is also well detected.*

Table 10: Result of the damage detection of the CLAS using PCA: damage 2

	$\mathrm{DI}_{\mathrm{PCA}}$	$\mu_{\beta,\mathrm{PCA}}$
Damage2 of the CLAS: delamination of an antenna network	0.4292	0.0347

In order to consolidate our results, we have performed other tests of the healthy and the damaged (damage 2) state of the CLAS using PZT 3 as an actuator. To test the damage detection methodology regarding the alarm false, we have done other tests of the healthy state (tests1-4); with enough time lags between them. Figure 12 depicts the damage rate versus the test number. We can observe that the damage rate is greater than one for the damaged states. One can also see that no false-positive alarms (NFPA) were detected.

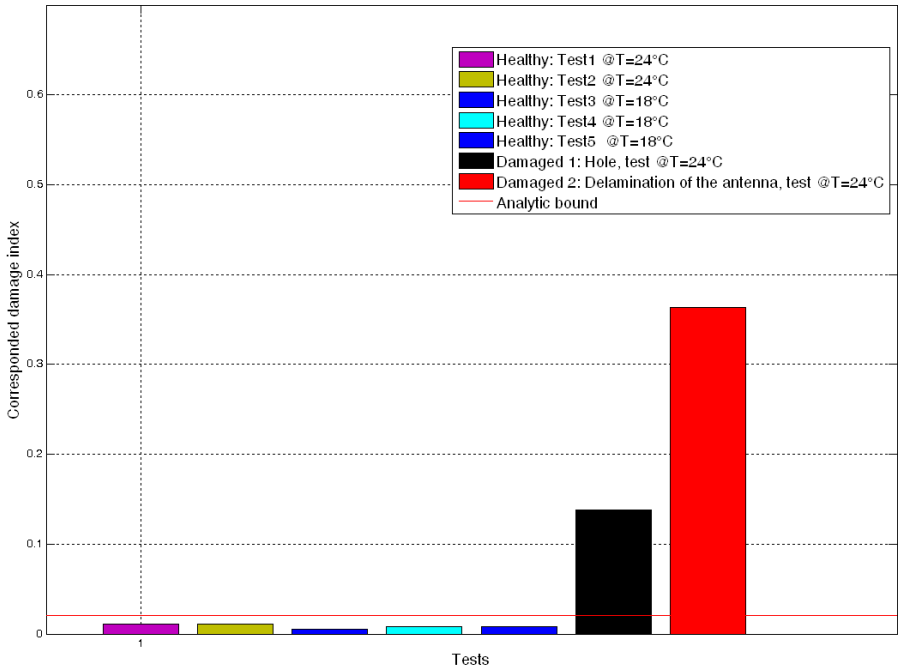

Figure 12: Application of the damage detection methodology using PCA and matrix perturbation for a CLAS structure

7. *Conclusion*

The important objective of a damage detection algorithm is to ascertain with efficiency the presence of damage. This decision can be done using a statistical model associated with the damage index. However, this model is an approximation due to the finite number of available baseline data. In this paper, we have explored the use of matrix perturbation theory (MPL) in the context of SHM.

Through this paper, we have proposed first a damage index based upon the change of the principal angle vectors between subspaces. This damage index does not require the knowledge of the mechanical model of the structure. So, it can be applied to more complex structures. To enhance the decision on the presence or not of damage, we have associated to this DI a bound. This later is entirely analytical, and it is suitable for adaptive damage diagnosis. This adaptability was tested to tackle the effect of temperature on a FE composite plate. Several changes of stiffness for the simulation setup and real delamination for the CLAS were well detected, with no false-positive alarms. Experiments on temperature effect (using enclosed heated space) and changes in boundary conditions are underway.

Acknowledgement

This work was supported by the project: Smart Materials and Structures for Electromagnetics funded by the consortium ASTech Ile de France. The authors wish to thanks all the persons involved in this project.

References

[1] N. Mechbal and E. Nobrega, "Damage Tolerant Active Control: Concept and State of the Art," *8th IFAC Symposium on Fault Detection, Supervision and Safety of Technical Processes. Mexico City, Mexico*, 2012.

[2] A. J. Lockyer, K. H. Alt, J. N. Kudva, R. W. Kinslow, and A. C. Goetz, "Conformal Load-Bearing Antenna Structures (CLAS): Initiative for Multiple Military and Commercial Applications," SPIE Conference on Smart Structures and Materials.California, USA: 1996.

[3] C. K. Kim, L. M. Lee, H. C. Park, W. Hwang, and W. S. Park, "Impact damage and antenna performance of conformal load-bearing antenna structures," *Smart Materials and Structures*, vol. 12, no. 5, pp. 672-679, 2003.

[4] P. J. Callus, "Conformal Load-Bearing Antenna Structure for Australian Defence Force Aircraft," Air Vehicles Division. Defence Science and Technology Organisation. Australia,DSTO Technical Report, 40, DSTO-TR-1963, 2007.

[5] MSIE, "State of the Art for the Projet MSIE: Smart Materials and Structures for Electromagnetics," *Document INE-MSI_DE-0004-A. Paris, France*, 2009.

[6] V. Giurgiutiu, B. Xu, and W. Liu, "Development and Testing of High-Temperature Piezoelectric Wafer Active Sensors for Extreme Environments," *Structural Health Monitoring*, vol. 9 (6) : 513-525 2010.

[7] W. J. Staszewski and A. N. Robertson, "Time-Frequency and Time-Scale Analyses for Structural Health Monitoring," *Philosophical Transactions of the Royal Society A: Mathematical, Physical and Engineering Sciences*, vol. 365 (1851): 449-477 2007.

[8] F. K. Chang, J. F. C. Markmiller, J. B. Ihn, and K. Y. Cheng, "A Potential Link from Damage Diagnostics to Health Prognostics of Composites Through Built-in Sensors," *Journal of Vibration and Acoustics, Transactions of the ASME*, vol. 129 (6): 718-729 2007.

[9] C. Boller, F. K. Chang, and Y. Fujino, *Encyclopedia of Structural Health Monitoring*. New York, USA: John Wiley & Sons, 2009.

[10] J. B. Ihn and F. K. Chang, "Detection and Monitoring of Hidden Fatigue Crack Growth Using a Built-In Pizoelectric Sensor/Actuator Network," *Smart Materials and Structures*, vol. 13 (3): 609-620 2004.

[11] H. Sohn, G. Park, J. R. Wait, N. P. Limback, and C. R. Farrar, "Wavelet-Based Active Sensing for Delamination Detection in Composite structures," *Smart Materials and Structures*, vol. 13 (1): 153-160 2004.

[12] J. N. Yang, Y. Lei, S. Lin, and N. Huang, "Hilbert-Huang Based Approach for Structural Damage Detection," *Journal of Engineering Mechanics*, vol. 130, no. 1, pp. 85-95, 2004.

[13] M. I. Friswell and D. J. Inman, "Sensor Validation for Smart Structures," *Journal of Intelligent Material Systems and Structures*, vol. 10, no. 12, pp. 973-982, 2000.

[14] P. De Boe and J. C. Golinval, "Principal Component Analysis of a Piezosensor Array for Damage Localization," *Structural Health Monitoring*, vol. 2 (2): 137-144 2003.

[15] R. Hajrya, N. Mechbal, and M. Vergé, "Proper Orthogonal Decomposition Applied to Structural Health Monitoring," *IEEE International Conference on Communications, Computing and Control Applications. Hammamet, Tunisia*, 2011.

[16] I. T. Jolliffe, *Principal Component Analysis*. New York, USA: Springer, 1986.

[17] A. Hyvärinen, J. Karhunen, and E. Oja, *Independent Component Analysis: Algorithms and Applications*. New York, USA.: John Wiley & Sons, 2001.

[18] P. Comon and C. Jutten, "Handbook of Blind Source Separation," Elsevier Ltd. Burlington, USA: 2010.

[19] L. E. Mujica, J. Rodellar, A. Fernández, and A. Güemes, "Q-Statistic and T2- Statistic PCA-Based Measures for Damage Assessment in Structures," *Structural Health Monitoring*, vol. 10, no. 5, pp. 539-553, 2011.

[20] G. Kerschen, P. De Boe, J. C. Golinval, and K. Worden, "Sensor Validation Using Principal Component Analysis," *Smart Materials and Structures*, vol. 14 (1): 36-42 2005.

[21] G. M. Stewart and J. G. Sun, *Matrix Perturbation Theory*. Boston, USA: 1990.

[22] J. F. Cardoso, "The Three Easy Routes to Independent Component Analysis, Contrasts And Geometry," In: Proceedings of ICA 2001. San Diego, USA, 2001.

[23] T. M. Cover and J. A. Thomas, *Elements of Information Theory*, 2nd Edition ed. John Wiley & Sons. New Jersey, USA: 2006.

[24] A. Hyvärinen, "Independent Component Analysis Using Mutual Information," *Report N° A 46, Department of Computer Science, University of Helsinki, Finland*, 1997.

[25] S. Valle, W. Li, and S. J. Qin, "Selection of the Number of Principal Components: The Variance of the Reconstruction Error Criterion with a Comparison to Other Methods," *Industrial and Engineering Chemistry Research*, vol. 38 (11): 4389-4401 1999.

[26] G. H. Golub and C. F. Van Loan, *Matrix Computation* Johns Hopkins University Press. Baltimore, USA, 1983.

[27] C. Davis and W. M. Kahan, "The Rotation of Eigenvectors by a Perturbation," *SIAM Journal on Numerical Analysis*, vol. 7 (1): 1-46 1970.

[28] P. Wedin, "Perturbation Bounds in Connection with Singular value Decomposition," *Numerical Mathematics*, vol. 12(1): 99-111 1972.

[29] R. Hajrya, "Contrôle Santé des Structures Composites : Approche Expérimentale et Statistique." PhD Thesis. École Nationale Supérieure d'Arts et Métiers. Paris, France, 2012.

[30] R. Hajrya, N. Mechbal, and M. Vergé, "Active Damage Detection and Localization Applied to a Composite Structure Using Piezoceramic Patches," *IEEE Conference on Control and Fault-Tolerant Systems. Nice, France*, 2010.

[31] E. Balmes, J. E. Bianchi, and J. M. Leclère, "Structural Dynamics Toolbox User's Guide," Paris, France: 2008.

[32] Ferroperm, "Material Data Based on Typical Values for Piezoceramic," http://www. *ferroperm-piezo. com/*, 2009.